Aerodynamics performance of a ventilation system for droplets controlling by coughing in a hospital isolation ward

Yunfei Song
Wuhan University
Chengqing Yang
Wuhan Pulmonary Hospital
Hui Li (li_hui@whu.edu.cn)
Wuhan University https://orcid.org/0000-0002-4404-8845
Hongbin Chen
Renmin Hospital of Wuhan University: Wuhan University Renmin Hospital
Shengnan Shen
Wuhan University
Yuqing Hou
Wuhan University
Jiayue Wang
Wuhan University

Research Article

Keywords: Computational fluid dynamics (CFD), Virus airborne diffusion, Local exhaust ventilation system

Posted Date: June 3rd, 2022

DOI: https://doi.org/10.21203/rs.3.rs-1640774/v1

Aerodynamics performance of a ventilation system for droplets controlling by coughing in a hospital isolation ward

Yunfei Song [1], Chengqing Yang [2], Hui Li [1,3,4] (✉), Hongbin Chen [5] (✉), Shengnan Shen [4], Yuqing Hou [1], Jiayue Wang [1]

1. The Institute of Technological Sciences, Wuhan University, Wuhan 430072, China

2. Wuhan Pulmonary Hospital, Wuhan Institute for Tuberculosis Control, Wuhan 430030, China

3. Key Laboratory of Hydraulic Machinery Transients (Wuhan University), Ministry of Education, Wuhan 430072, China

4. School of Power and Mechanical Engineering, Wuhan University, Wuhan 430072, China

5. Pulmonary and Critical Care Medicine, Renmin Hospital of Wuhan University, Wuhan 430060, China

✉. Correspondence: li_hui@whu.edu.cn, 200413000024@whu.edu.cn

Abstract

Over 270 million people have been infected by the coronavirus disease 2019 (COVID-19) in the past two years, resulting in 5 million deaths. The virus primarily transmitted through droplets or aerosols produced by coughing, sneezing, and talking. A full-scale isolation ward in Wuhan Pulmonary Hospital is modeled in this work, and water droplet diffusion is simulated using the Computational Fluid Dynamics (CFD) approach. In an isolation ward, a local exhaust ventilation system is intended to avoid cross-infection. The existence of a local exhaust system increases turbulent movement, leading to a complete breakup of the droplet cluster and improved droplet dispersion inside the ward. When outlet negative pressure is 4.5 Pa, the number of moving droplets in the ward decreases by approximately 30% compared to the original ward. The local exhaust system could minimize the number of droplets evaporated in the ward; however, the formation of aerosols cannot be avoided. Furthermore, in six different scenarios there are 60.83%, 62.04%, 61.03%, 60.22%, 62.97% and 61.52% droplets produced by cough deposited on the surface of the patient. However, the local exhaust ventilation system has no apparent influence on the control of surface contamination. This study provides several suggestions for the optimization of ventilation in the wards, and scientific evidence to ensure the air quality of hospital isolation wards.

Keywords Computational fluid dynamics (CFD), Virus airborne diffusion, Local exhaust ventilation system

Introduction

The study of airborne diseases has been increasingly significant, recently, with the emergence of severe acute respiratory syndrome, Ebola virus, tuberculosis, coronavirus disease 2019 (COVID-19), and other infectious diseases (Hathway et al. 2011). With the outbreak of the COVID-19 worldwide (as of January 20, 2022), there have been 332,617,707 people diagnosed with COVID-19, including 5,551,314 deaths globally (WTO 2022). Some countries or regions adopted closed-off management to prevent the spread of the disease, which seriously affected economic growth and the normal operation of the whole city. Over the last two years, countries have prioritized preventing and controlling the epidemic. Every day, 10,000 people worldwide die as a result of COVID-19. It can affect anyone anywhere, especially the healthcare workers exposed to the environment existing virus droplets. Therefore, the study of virus airborne diffusion in hospital isolation rooms is significant.

Viral respiratory infections are diffused by contact and droplet transmission, fomite transmission, and other types of transmission (WTO 2020). Contact transmission occurs when a healthy man is in close contact with a person who is infected (direct contact) or when an infected individual exhaust fomites containing viral droplets (indirect contact) (Morawska et al. 2020). Viruses spread through the air via droplets or aerosols produced during coughing, sneezing, and talking (Jones et al. 2015). As an intense process of droplet generation for transient time, recently the focus of study has been on cough. Small virus droplets expelled into the air can exist as airborne for a long time (WTO 2009) and can fill the whole room under the effect of an air conditioner (Liu 2020). Li et al. (2020) investigated the spread of droplets in the tropical outdoor environment and found that at wind speeds of 2 m/s, 100 μm droplets can move up to 6.6 m. Wei et al. (2015) modeled the coughing process as a turbulence jet to investigate diffusion of droplets and obtained travel distances with different droplet sizes. Lindsley et al. (2016) compared aerosol droplets samples of 61 adult volunteer outpatients through experiments and found that more aerosol droplets containing viruses were released by coughing. Nicas et al. (2005) analyzed the pathogen-containing droplet emission from an infected person, and results indicated that the droplets are composed of 98.2% water and 1.8% of nonvolatile solid compounds.

Furthermore, COVID-19 outbreak can spread from one room to another via a ventilation system. Nissen et al. (2020) investigated the ventilation system in a COVID-19 isolation unit at Uppsala University Hospital through an experiment. They found that the virus could spread long distances via central ventilation systems. And other researches had also found viral RNA in samples from ventilation systems in isolation rooms (Guo et al. 2020; Liu et al. 2020). Thus, long distances airborne dispersal of COVID-19 virus in hospital wards exist and significantly increases cross-infection risk.

Computational fluid dynamics (CFD) has been widely utilized to analyze the mobility of droplets indoors. Davardoost and Kahforoushan (2019) simulated the dispersion of volatile organic compounds indoor via CFD modeling to investigate the performance of ventilation. Liu et al. (2020) used a full-experimental and numerical simulation to investigate the transmission and deposition of bioaerosols in a hospital isolation ward in which the Re-Normalisation Group (RNG) k-ε model was selected. Bhattacharyya et al. (2020) studied the flow field in an isolation ward when both air-conditioning system and sanitizing machine kept working through CFD method in which transition

SST k-ε model was applied. They found that the high turbulent fields generated in the ward may be conducive to the spread of sanitizer. Borro et al. (2020) used the CFD method to investigate the droplet diffusion from a coughing event in the waiting room and recovery ward of Vatican State Children's Hospital, and the RNG k-ε model was employed in numerical simulation. Results indicated that ventilation system accelerated the spread of infected droplets across in the whole waiting room and the local exhaust ventilation system could help to remove the contaminated air. Li et al. (2020) investigated the diffusion of droplets generated from the patient's wound under four different ventilation systems during the surgery through CFD method and obtained the optimal arrangement of the ventilation system. Cho (2018) evaluated the flow field of contaminated droplets exhaled from patients in an isolation ward at three different ventilation systems and obtained an improved ventilation system using numerical simulation and field measurement, which efficiently removed contaminated droplets.

Although extensive study has been conducted on the simulation of droplets dispersion from a coughing episode and contaminant dispersal throughout the ward, there has been little research on the fast removal of contamination sources in an isolation ward. The main objective of this work is to analyze propagation characteristics of droplets containing viruses induced by coughing in the ward and to design a local exhaust ventilation system to control droplets diffusion. A full-scale experiment is conducted to verify the flow field. The temporal and spatial distribution of droplets in six scenarios are simulated through the CFD method. Additionally, the number of moving, evaporated, and deposited droplets is quantitatively analyzed. This study provides several guidelines for optimizing ventilation in hospital wards, and scientific evidence for ensuring the air quality of hospital isolation wards.

Problem description

The main transmission route of infection is that viruses spread through the air via droplets or aerosols produced during coughing, sneezing, and talking (Jones et al. 2015). A high concentration of contaminated droplets in the hospital epidemic ward raises the danger of infection from patients to health care staff as well as patient cross-infection. A ventilation system ensures the air quality indoors and protects healthcare workers and patients from contaminants (Liu et al. 2020). Therefore, it is important to design an effective ventilation system to reduce droplet diffusion in the hospital wards. Based on the above questions, coughing and droplets release processes in the isolation ward of Wuhan Pulmonary Hospital are simulated through the CFD method to improve the ventilation system's performance. The geometric model is established based on the actual measurement of the isolation ward in Wuhan Pulmonary Hospital as shown in Fig. 1.

According to Zhu et al. (2020), Yao et al. (2020), and Ke et al. (2020), COVID-19 was an enveloped virus with a large nucleoprotein, and virions ranging in size from 60 to 140 nm. Furthermore, Bi et al. (2021) discovered that the diameter of cough followed by the Rosin-Rammler distribution, with an average diameter of 0.02 mm. Compared with the droplets, the size of virions can be ignored since they are tiny. We assume that all droplets contain viral droplets to simplify the model in the simulation. The material of droplets is simplified as water according to the investigation of Nicas et al. (2005). The droplets are injected from the patient's mouth in the time range of 0.042-0.136 s and the cough velocity can reach 22.06 m/s in a short period (Borro et al. 2020; Gupta et al. 2011), as shown in Fig. 2. Droplets properties used in the simulation are shown in Table 1.

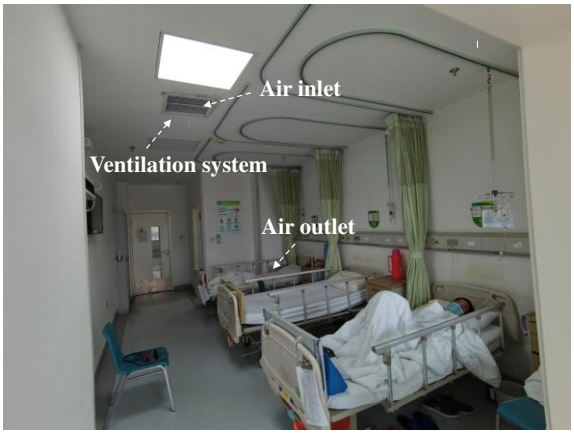

Fig. 1 Layout of an isolation ward in Wuhan Pulmonary Hospital.

Table 1. Droplets properties used in discrete phase model (Nicas et al. 2005; Borro et al. 2020; Gupta et al. 2011)

Material	Diameter distribution	Diameter (mm)	Velocity (m/s)	Temperature (K)
H_2O	Rosin-Rammler	0.002~0.1	22.06	310

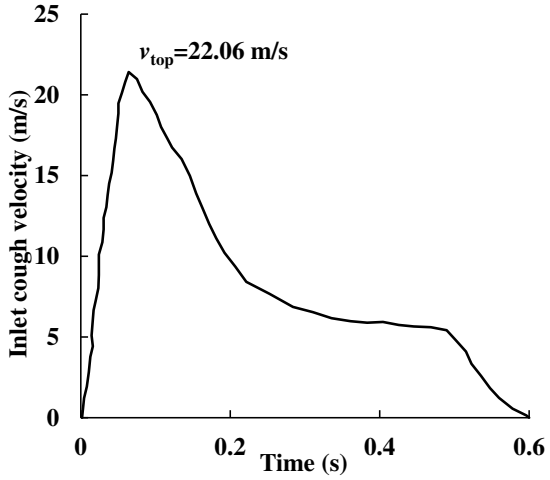

Fig. 2 Velocity profile of one cough by patient [13].

Method

Geometry and mesh

The geometric model is established based on the actual measurement of the isolation ward in Wuhan Pulmonary Hospital. The patient's geometry has made some necessary simplifications to reduce the computational cost. There is a naturally ventilated air outlet near the bed, and a ventilation system located on the ceiling delivers fresh air to the ward. The patient is placed in the middle bed in this model. Fig. 3 plots the schematic of the ward and the furniture's dimension.

The meshes are generated using the Gambit (ANSYS, Gambit 2.4.6, Canonsburg, PA, USA). The hybrid grid method is used in the gridding drawing process. The meshes of the furniture zone are

generated using tetrahedron elements to ensure the quality of the mesh, which is shown in Fig. 4(a). Furthermore, the structured grid is used in the regular fluid zone to reduce the amount of calculation. Therefore, the meshes surrounding the patient are defined as plotted in Fig. 4(b) and Fig. 4(c) from the cross-section M-M and N-N respectively. The whole zone of fluid consists of tetrahedron and hexahedron elements with 5,807,108. In our previous work (Cai et al. 2016; Zhang et al. 2015; Song et al. 2021), the same method generates the model's mesh. In other words, the validity of the mesh has already been verified.

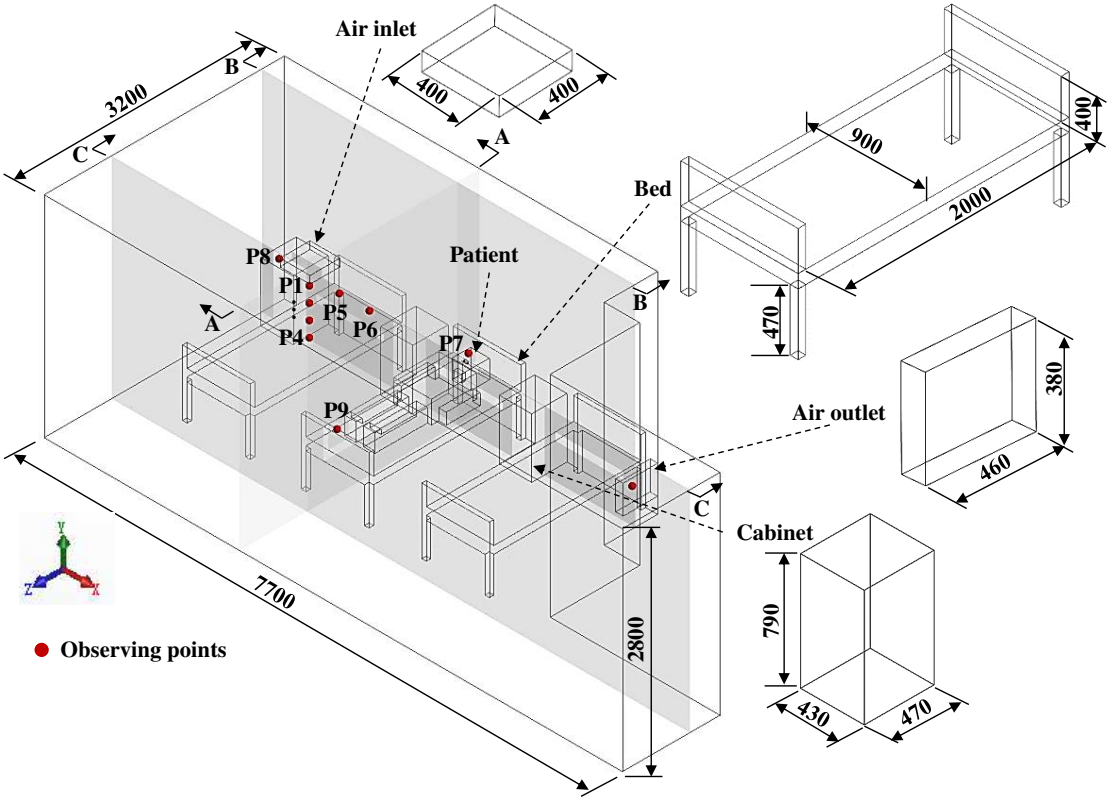

Fig. 3 Schematic of the ward and the dimension of furniture (unit: mm).

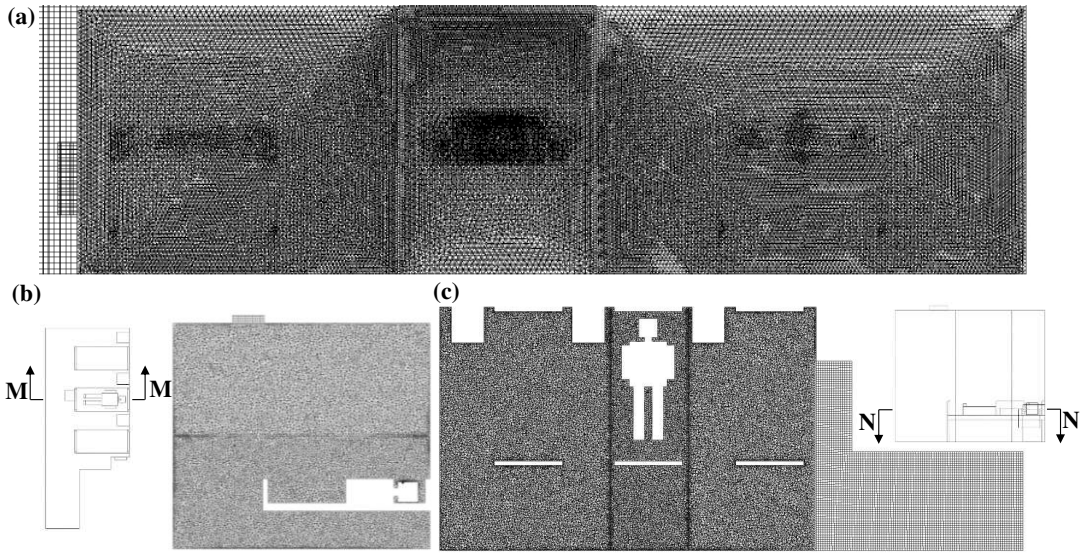

Fig. 4 Meshes for the CFD simulation (a) mesh of the furniture, (b) mesh of the manikin on the cross-section M-M, (c) mesh of the manikin on the cross-section N-N.

Airflow modeling

The flow field is simulated using the CFD solver ANSYS Fluent (Fluent 2020 R2, ANSYS, Canonsburg, PA, USA). To simulate the indoor turbulence flow field, three turbulence models are extensively used: Reynolds Average Navier-Stokes (RANS), direct numerical simulation (DNS), and large eddy simulation (LES) (Choi et al. 2012; Wang et al. 2018). In the indoor flow field simulation, the DNS and LES require longer computation times and more computer capacity than the RANS. Considering the accuracy and amount of the calculation, the RANS equations are used (Chen et al. 1995).

The continuity and the Navier-Stokes equation can be written as follows:

$$\frac{\partial \overline{u}_m}{\partial x_m} = 0 \tag{1}$$

$$\frac{\partial u_m}{\partial t} + \frac{\partial (\overline{u}_m \overline{u}_n)}{\partial \overline{u}_n} = -\frac{1}{\rho}\frac{\partial \overline{P}}{\partial x_m} + \nu \frac{\partial^2 \overline{u}_m}{\partial x_n x_n} + \frac{\partial \tau_{mn}}{\partial x_n} \tag{2}$$

where u_m is the fluid velocity in the m direction, x_m is the coordinate in the m direction, and P represents the pressure of the fluid. The overbar in the equations denotes the mean variables. And the τ_{mn} is the Reynolds stress.

Because of cough, a turbulent jet event (Bourouiba et al. 2014), the RNG k-ε model in the RANS method is used in the simulation, which has been proved effective in the simulation of indoor turbulent flow field (Liu et al. 2020; Borro et al. 2020; Liu et al. 2017). This model is derived from renormalization theory, in which an additional term is added in the epsilon equation to improve the accuracy of turbulence flow (Abraham et al. 1997; Yakhot et al. 1986). For solving method, the pressure-implicit with splitting of operators algorithm is selected due to the suitability for transient flows.

Discrete phase

To simulate the diffusion of droplets from a cough, the discrete model is used. The droplet force balance equation in the discrete phase model theory is defined as (Fluent ANSYS 2020):

$$m_d \frac{d\vec{u}_d}{dt} = m_d \frac{\vec{u}_f - \vec{u}_d}{\tau_r} + \frac{m_d \vec{g}(\rho_d - \rho)}{\rho_d} + \vec{F} \tag{3}$$

where m_d represents the mass of droplet, $\vec{u}_f$ is the velocity of the fluid, $\vec{u}_d$ is the velocity of a droplet, $\vec{F}$ is an additional force and τ_r is the relaxation time of a droplet.

In the right-hand side of the equation, the term is the drag force; the second part represents a force under the influence of gravity; the third part is additional forces under various circumstances, such as forces in moving reference frames, thermophoretic force, Brownian force, Saffman's lift force, Magnus lift force and user-defined force.

Drag force and gravity have the greatest influence on the dynamic behavior of droplets formed by cough occurrences. The droplet motion is assumed as a stochastic collision. Other forces, including thermophoresis and Brownian forces, are too small to be ignored in the simulation. Therefore, droplets are mainly affected by the drag forces, generation of turbulence associated with

the ventilation system, and gravity force.

Evaporation of droplets

After exhaling infectious droplets through cough, small suspended droplets could form short-duration droplets cloud. Then, droplets could suspend via air in the ward for a long time. The surface of the droplet exchanges a lot of heat and mass with the ambient. In other words, a portion of the droplets evaporates into water vapor suspended indoors for a long time. Therefore, the evaporation process of the suspension droplets is of great significance in analyzing the risk of infectious droplet transmission. Kukkonen et al. (1989) proposed a model of pure water droplets evaporation and dispersion, driven by the partial pressure difference between the droplet surface and the ambient air. Many studies about droplets evaporation are currently based on this work (Mao et al. 2020).

The droplet is assumed to be uniform in this study, which means that there is no gradient in concentration or temperature within the droplet. Evaporation and convection are the main heat exchangers between the droplet surface and the ambient air. The radiation heat transfer can be neglected due to the minimal temperature difference. The temperature of the droplet changes is determined by Eq. (4) (Parienta et al. 2011).

$$m_d C_d \frac{dT_d}{dt} = \pi h_c D_d^{\,2} (T_\infty - T_d) + L_t \frac{dm_d}{dt} \tag{4}$$

where m_d is the mass of the droplet, C_d is the heat capacity of water, T_d is the droplet temperature, D_d is the droplet diameter, T_∞ is the ambient temperature and L_t is the latent heat of vaporization. The left part of the equation indicates the total enthalpy change in a droplet. On the right-hand side of the equation, the first part is the convection heat transfer between the air and the droplet's surface; the second part represents the latent by droplet vaporization.

And the heat transfer coefficient h_c in Eq. (4) can be obtained as (Chao et al. 2006):

$$Nu = \frac{h_c D_d}{k_g} = 2.0 + 0.6\,\mathrm{Re}_d^{1/2} + \mathrm{Pr}^{1/3} \tag{5}$$

where k_g is the thermal conductivity of air, Nu is the Nusselt number, Pr is the Prandtl number, and Re_d is the droplet Reynolds number.

Boundary condition

Before simulation, the inlet speed of the ventilation system is tested in Wuhan Pulmonary Hospital, and the speed obtained is 1.045 m/s. The air is set to 295 K, and the walls are assumed as adiabatic. Droplets are expected to be absorbed by surfaces (beds, cabinets, walls, and patient) as they collide with the surfaces due to their low momentum. Therefore, we select the trap as the boundary conditions of the surfaces. The other boundary conditions for CFD simulation are summarized in Table 2.

Table 2. Boundary conditions in the CFD simulation.

	Original	Ventilation_1	Ventilation_2	Ventilation_3	Ventilation_4	Ventilation_5
Ventilation outlet	/	Outlet pressure (Pa)				
		-2.5	-3.0	-3.5	-3.5	-3.5
		Outlet temperature: 300 K DPM condition: Escape				
Air inlet		Inlet velocity: 1.045 m/s Inlet temperature: 295 K DPM condition: Escape				
Air outlet		Outlet pressure: zero-gauge pressure Outlet temperature: 300 K DPM condition: Escape				
Droplet inlet		Droplet velocity: 22.06 m/s (in *Y* direction) Temperature: 310 K DPM condition: Escape				
Surfaces (beds, cabinets, walls, and patient)		Temperature: 300 K DPM condition: Trap				

Results and discussion

Validation of the flow filed

This study investigates the flow field and droplet diffusion in the isolation ward. Before conducting transient simulations, a stable scenario is simulated without the coughing process as the initial value to assure the airflow stability in the room. The CFD simulation results in the isolation ward are plotted below. Fig. 5 shows streamlines formed by the isolation ward's ventilation system. As shown in Fig. 5(a), the airflow from the inlet impacts the flow field in the isolation room. After the airflow hits the floor, one part of the airflow moves up the wall to the ceiling and forms a backflow zone, while the other part moves toward the empty area and returns. And after the vertical air reaches the floor, the airflow hits the bed and produces a recirculation region. Fig. 5(b) indicates flow field on the cross-section B-B. The airflow in the zone is observed to move toward the outlet, and a portion of the air hits the furniture and forms an eddy current area. Fig. 5(c) shows flow field on the cross-section C-C. After the air is delivered to the floor, the split flow reaches the floor and forms a backflow.

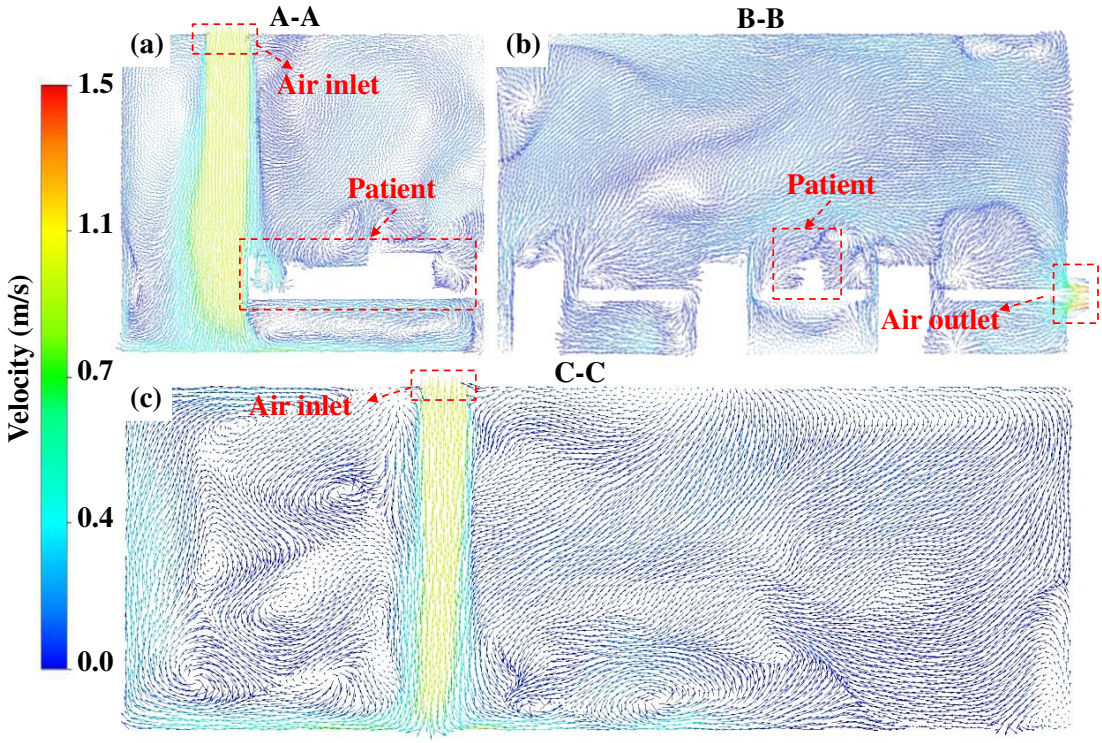

Fig. 5 Flow fields on the cross-sections (a) A-A, (b) B-B, and (c) C-C.

An experiment is conducted to measure velocities of 10 points to verify the flow field simulation. The measuring apparatus (Hot ball anemometer WS-40, Hongrui, China) is selected for measurement, placed in different positions to measure the velocity. The location of the observing points is illustrated in Fig. 2. And parameters of the WS-40 are summarized in Table 3. The test data can be collected in real-time and output to the laptop, as shown in Fig. 6.

During the experiment, the ventilation system is kept running. Furthermore, doors and windows are closed to separate the space from the outside world. In the process of the experiment, only the air-conditioning is turned on, resulting in no temperature change.

The velocity validation results at selected points are shown in Fig. 7. Results of the experiment and simulation are consistent. The mean absolute percentage error is less than 10%, indicating that the CFD simulation's boundary condition are suitable. Because the actual airflow is turbulent, using anemometers to measure velocity is difficult. In addition, in order to lower the computing cost, the simulation is simplified, which results in certain errors. But in this model, the errors between the simulation and the experiment are acceptable.

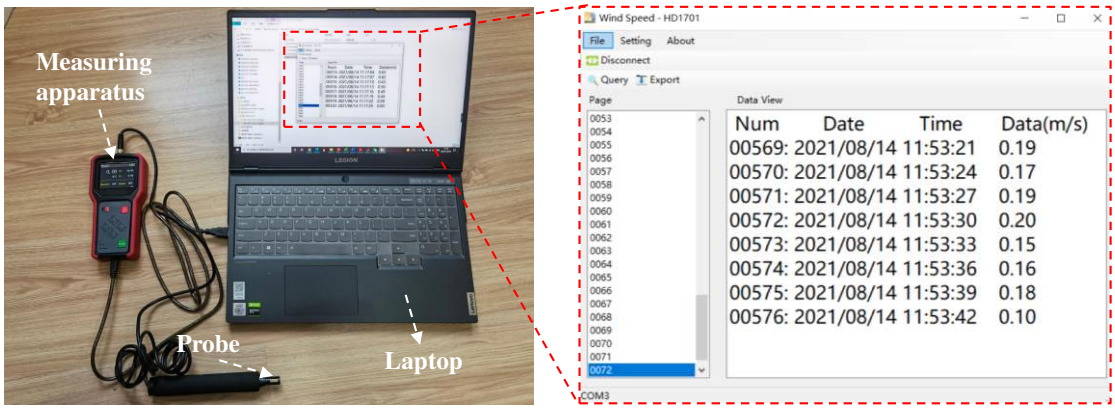

Fig. 6 Real-time acquisition of experiment data.

Table 3. Parameters of hot-bulb anemometer

	**Operating voltage**	**Temperature stability**	**Measurement range**	**Accuracy**
	3.7 V	0~50℃	0~2 m/s	0.01 m/s

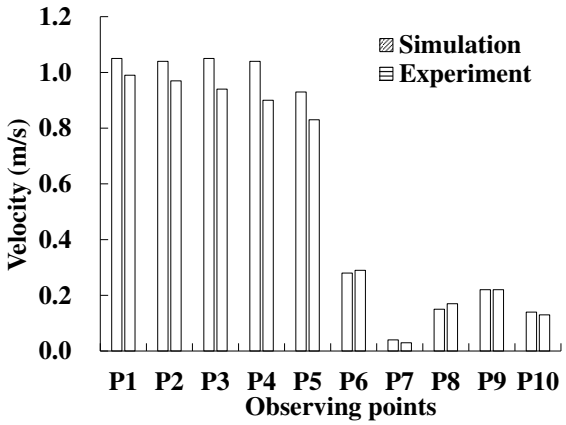

Fig. 7 Velocity validation at selected points.

Diffusion and distribution of Droplets

To investigate the droplets diffusion in the isolation ward, a steady scenario is simulated without the coughing process to ensure airflow stability in the room before releasing droplets. When the flow field in the room tends to be stabilized, droplets begin to be released (which means the patient starts coughing), and at this time t = 0 s. Fig. 8 shows the flow fields of one cough on the cross-section B-B in the original ward and Fig. 9 plots the temporal and spatial distributions of the droplets in the ward of Wuhan Pulmonary Hospital. At 0.1 s, a small portion is diffused to exhaust under the action of the flow field, which can be seen in Fig. 9; most droplets gather to form a droplet cloud. Droplets disperse gradually because of the vortex around the patient. These droplets hit the ceiling and continue to move along the wall, which can be observed at 0.3-2.0 s in Fig. 9. And flow fields on the cross-section B-B at 0.3 s and 0.6 s in Fig. 8 can explain the diffusion of droplets. Droplets begin to spread to the entire room at 3.0 s, affected by the eddy and buoyancy. Most droplets are eventually deposited on the patient surface and the walls, and a small portion can be observed to spread in the ward, which could carry virous and suspend indoors for a long time.

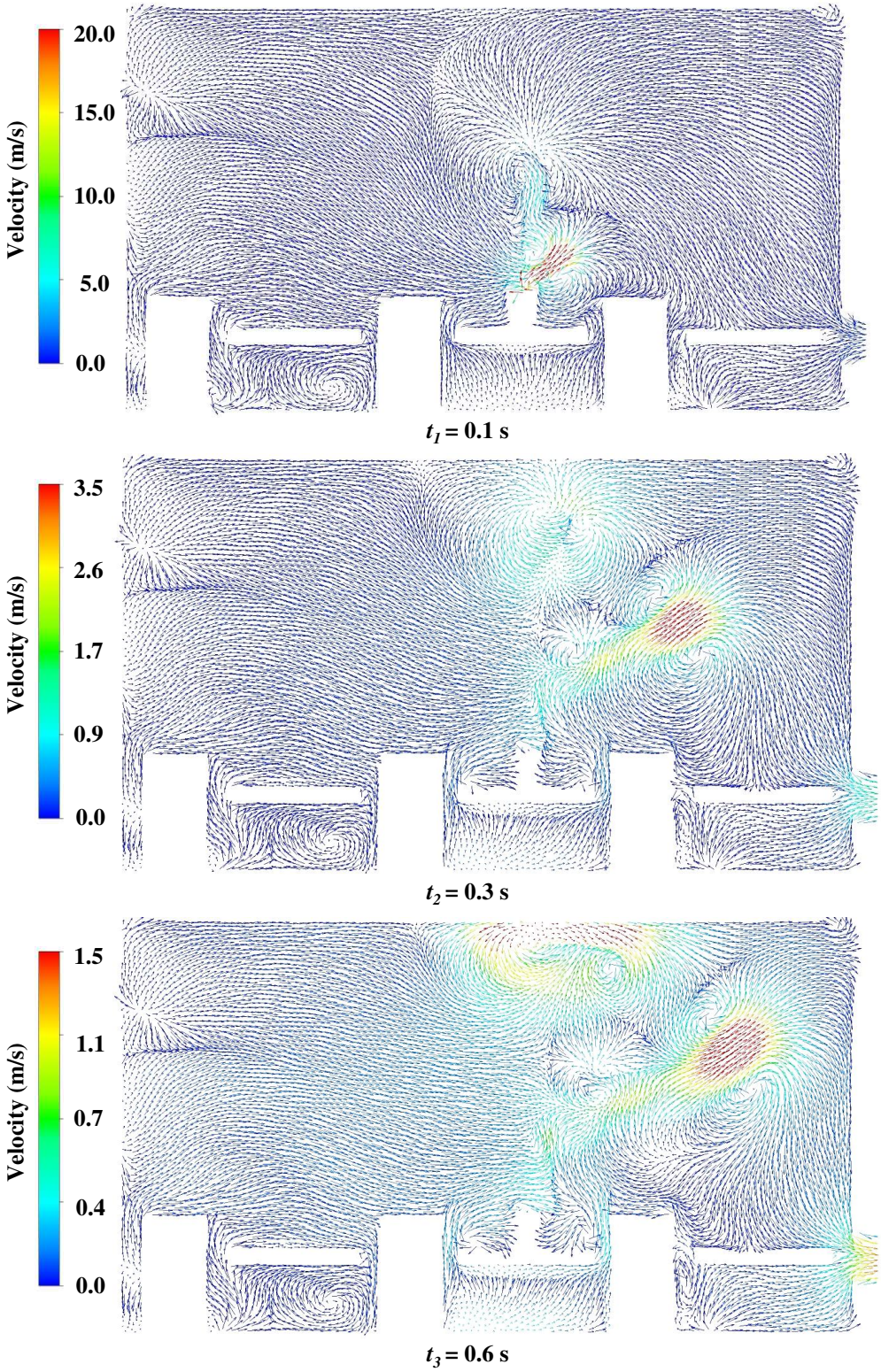

Fig. 8 Flow fields of one cough on the cross-section B-B in the original ward.

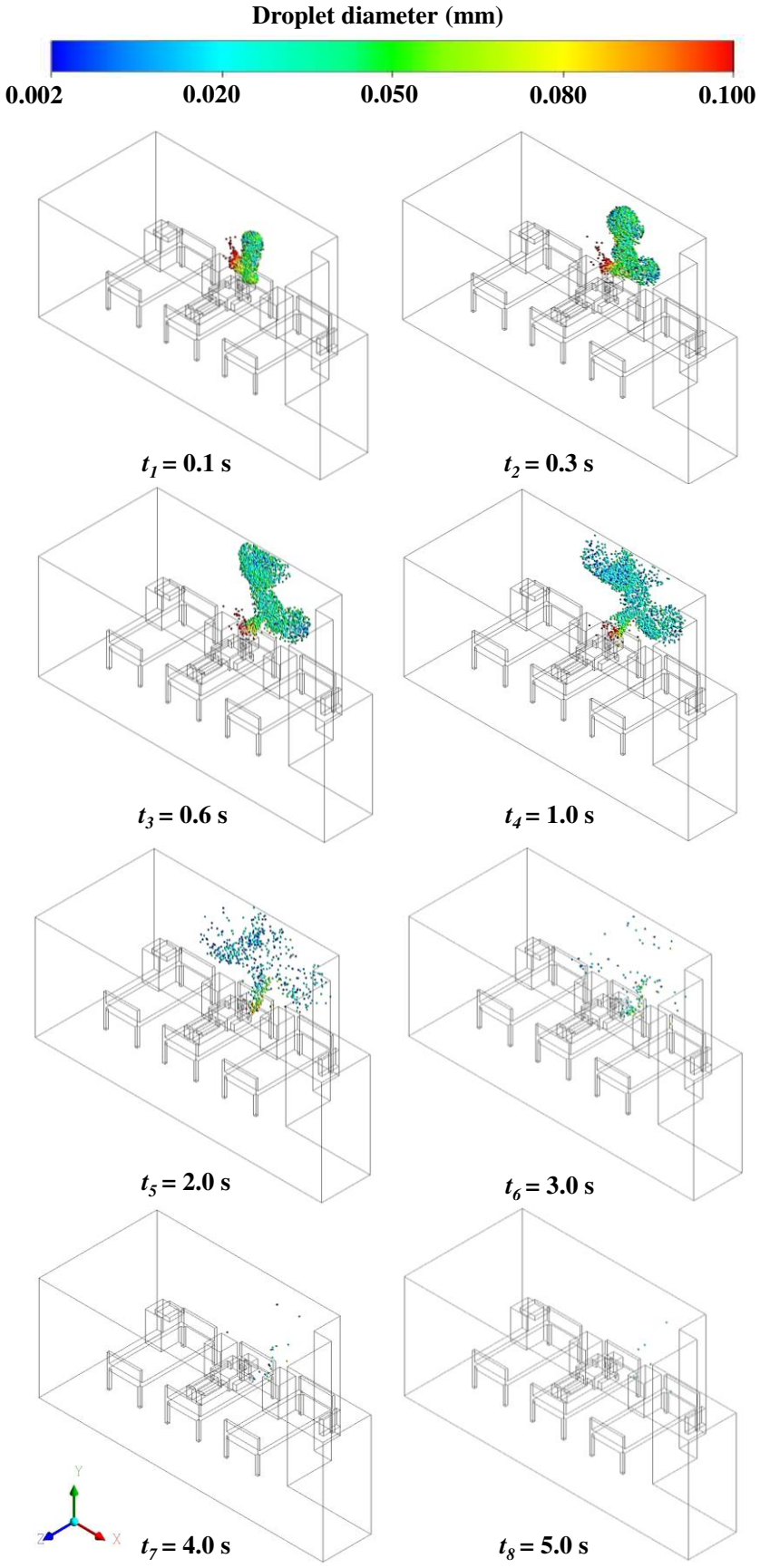

Fig. 9 Temporal and spatial distributions of droplets in the original ward.

Local exhaust ventilation system

As a fast-spreading infectious disease, the droplets containing the virus can remain in the room for a long time. The negative pressure ventilation systems isolate pathogenic droplets in hospitals, such as Wuhan Leishenshan Hospital (Luo et al. 2020). The layout of negative pressure wards can also minimize the exposure of patients and health care professionals to COVID-19 (Al-Benna 2021). According to the US Ventilation of Health Care Facilities, the minimum differential pressure between wards and relatively clean areas is 2.5 Pa (ANSI/ASHRAE/ASHE 2017). A local exhaust ventilation system is designed to ensure the air quality of the isolation ward, which is placed above the patient's head. The geometry of the ward furnished with the ventilation system and the dimension of the system is shown in Fig. 10.

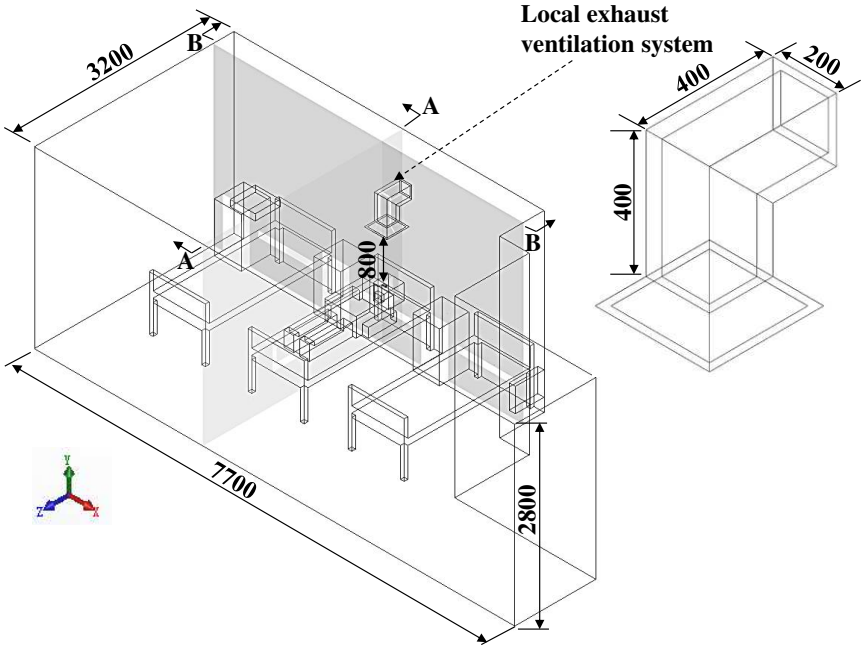

Fig. 10 Schematic of the isolation ward (unit: mm) furnished with the local exhaust ventilation system.

The initial outlet negative pressure of the local exhaust ventilation system is set at 2.5 Pa in scenario ventilation_1, and the other boundary conditions for CFD simulation are summarized in Table 2. The purpose of the simulation is to analyze the effect of the local exhaust system on droplet diffusion. Fig. 11 shows the flow field on the cross-section B-B. Coughed stream of contaminated air spread droplets, affect by the local exhaust system at 0.1 s. The droplet swarm is divided into two streams affected by the local exhaust device and the air outlet. The local exhaust system enhances the turbulent transport throughout the ward, compared with the original ward.

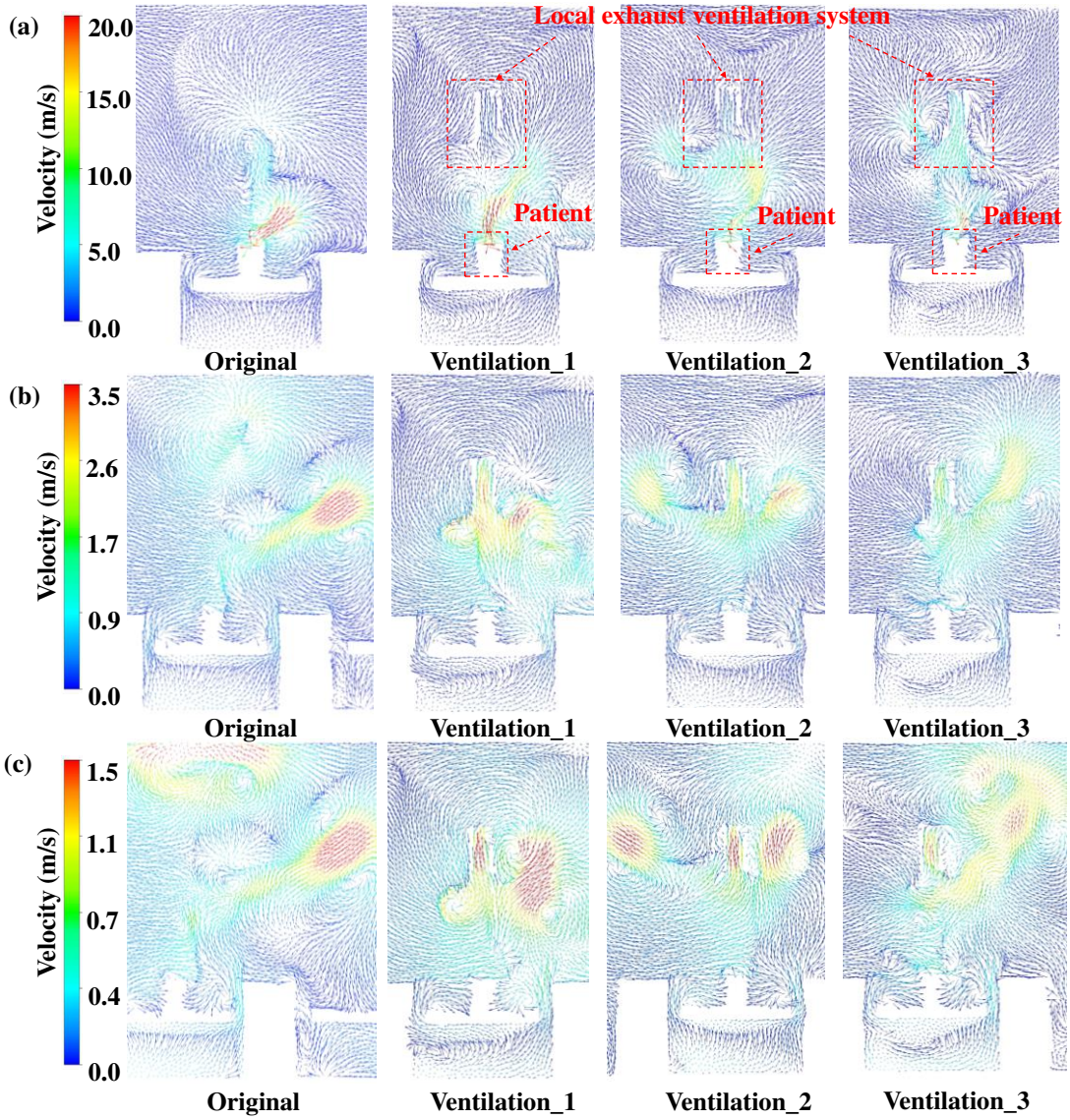

Fig. 11 Flow field of one cough on the cross-sections B-B in four scenarios at (a) t_1 = 0.1 s, (b) t_2 = 0.3 s, and (c) t_3 = 0.6 s.

The temporal and spatial distributions of droplets in the ward furnished a local exhaust ventilation system is plotted in Fig. 10. Interestingly, the existence of the local exhaust system promotes turbulent transport around the patient's head, leading to a complete breakup of the droplet cluster and enhancing the droplets' dispersion indoors. At 5.0 s, few droplets can be tracked moving in the ward, which means that most droplets are deposited or escape from the outlet.

In addition, we simulate droplet diffusion under different outlet negative pressures in scenario ventilation_2 and scenario ventilation_3. Fig. 13 and Fig. 14, respectively illustrates the temporal and spatial distributions of the droplets indoors. With an increase in the negative pressure, the local exhaust ventilation system can exhaust more droplets containing pathogenic microorganisms. However, the existence of the local exhaust ventilation system cannot remove all droplets thoroughly. Vortices can form in the area around the ventilation system, resulting in a portion of droplets contained in the room and moving with the indoor air.

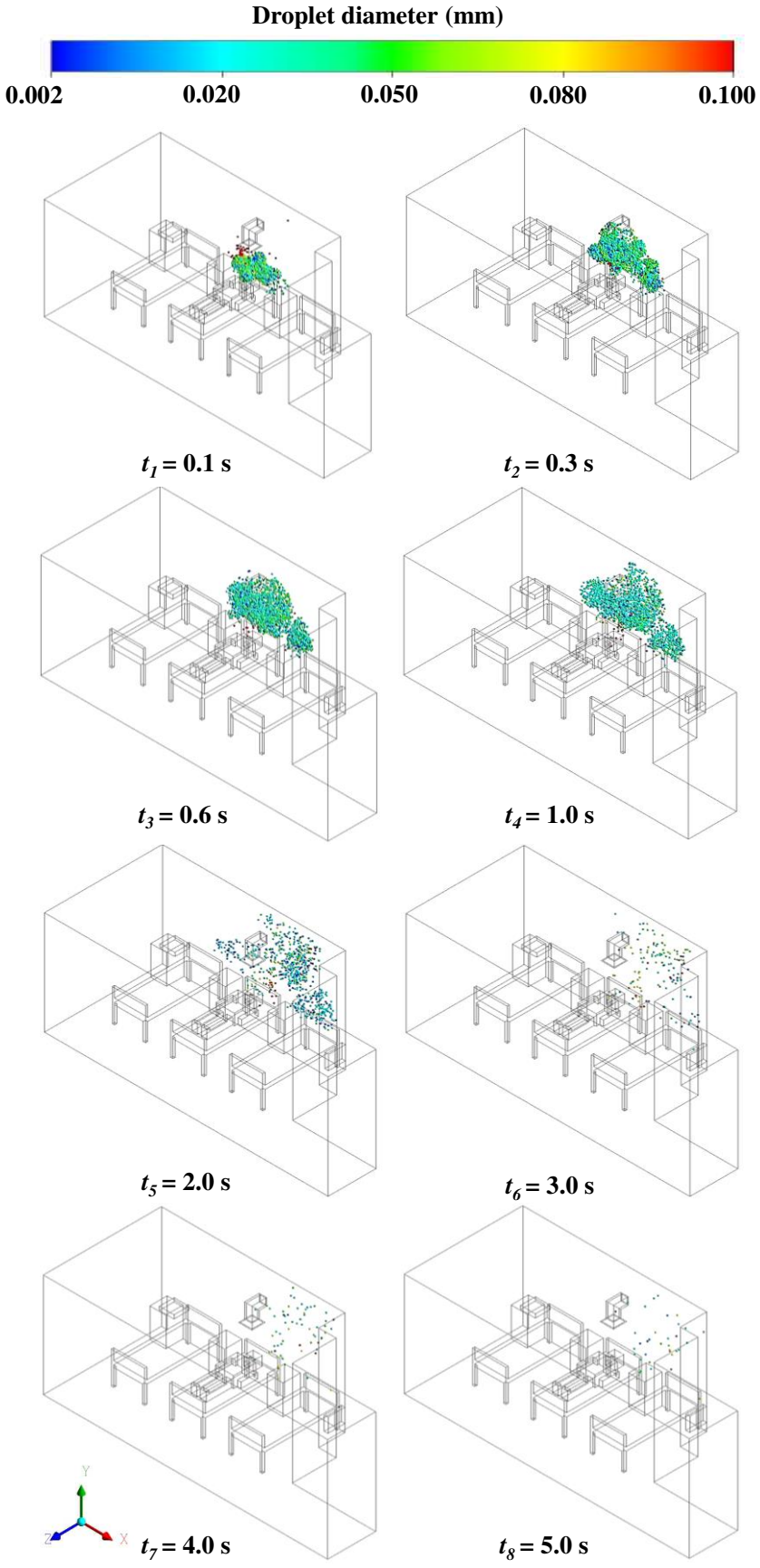

Fig. 12 Temporal and spatial distributions of droplets with designed local exhaust ventilation system when outlet negative pressure is 2.5 Pa.

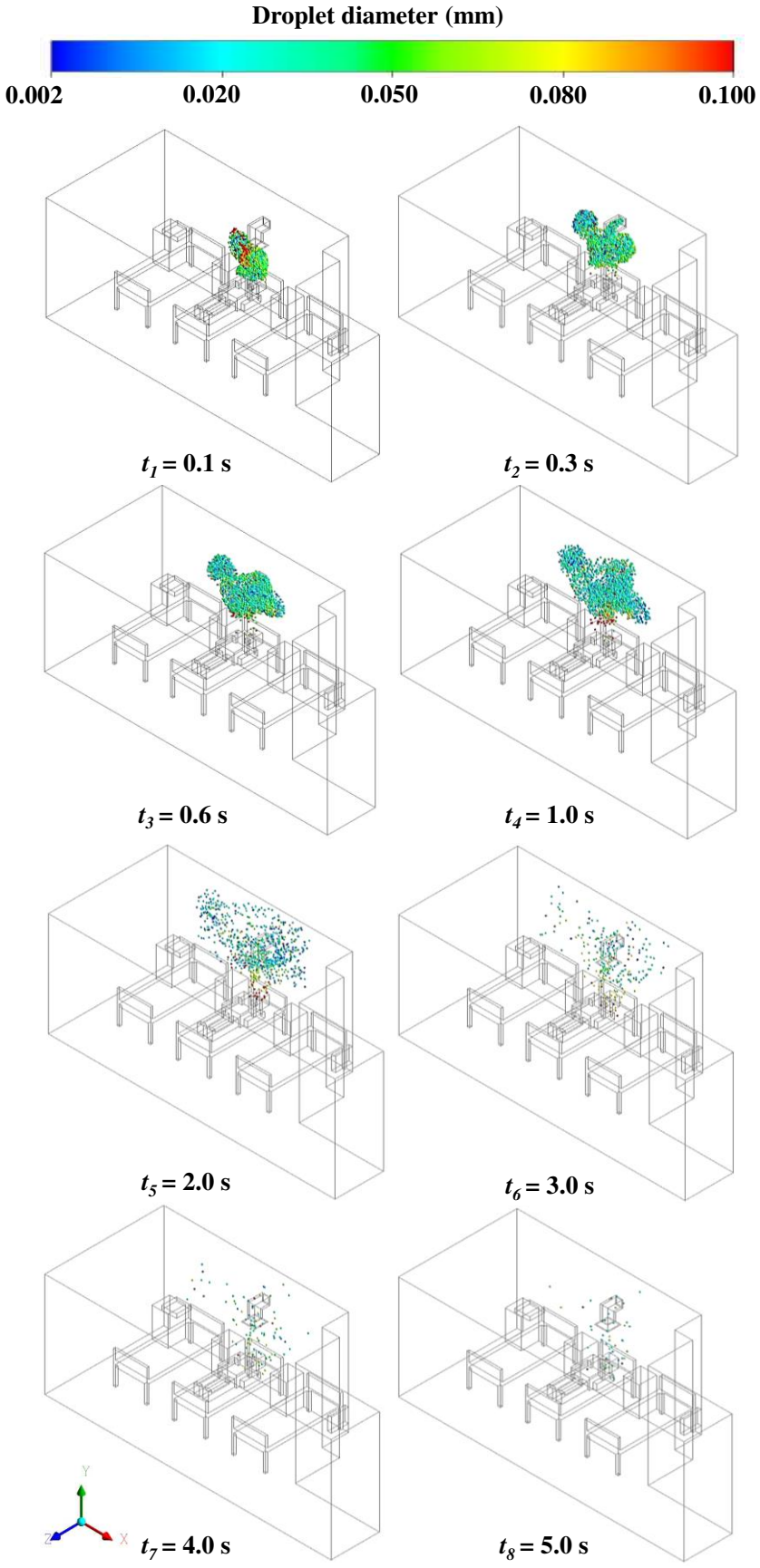

Fig. 13 Temporal and spatial distributions of droplets with designed local exhaust ventilation system when outlet negative pressure is 3.0 Pa.

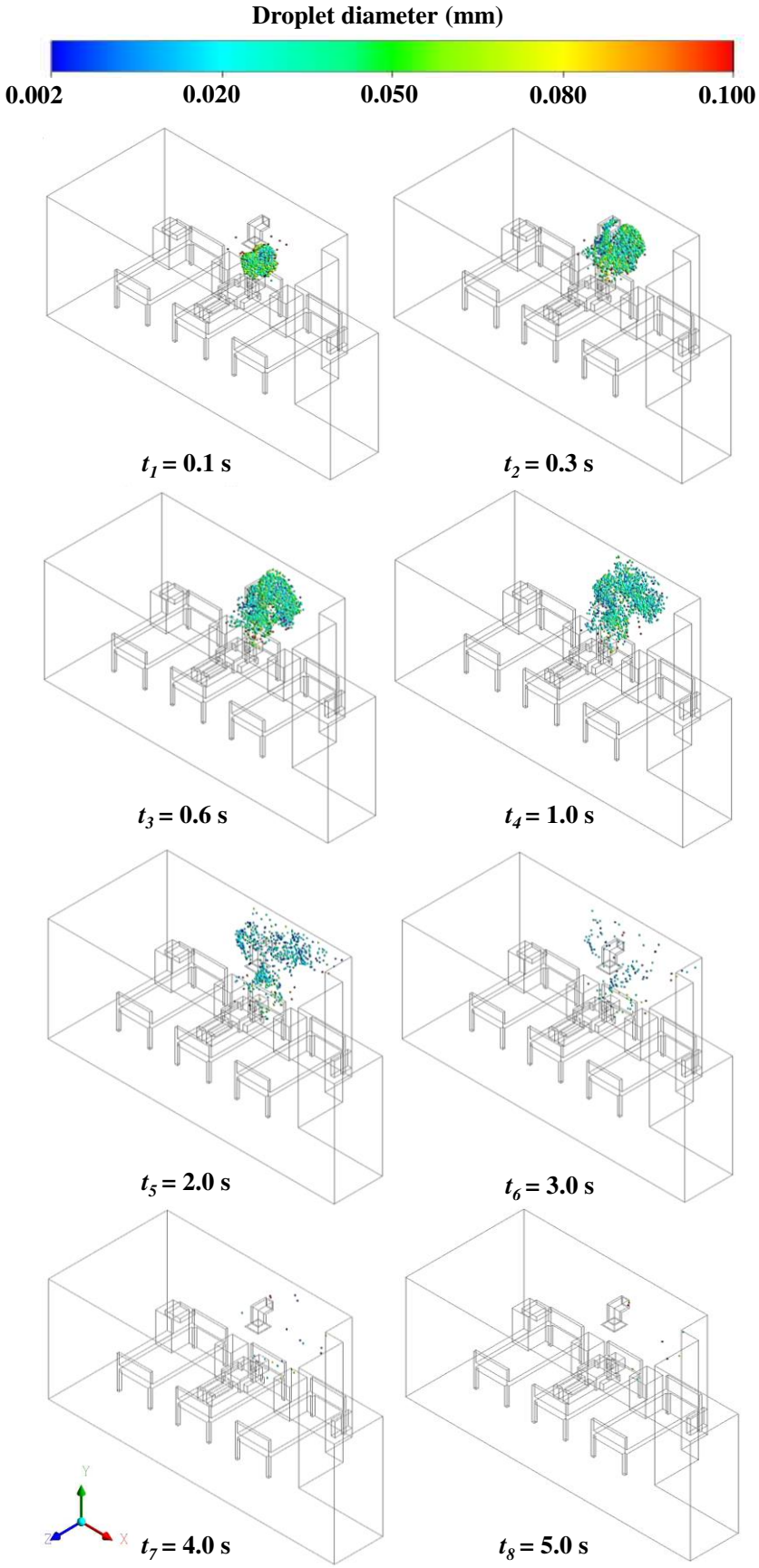

Fig. 14 Temporal and spatial distributions of droplets with designed local exhaust ventilation system when outlet negative pressure is 3.5 Pa.

To obtain the influence of the outlet negative pressure on droplet diffusion, two more scenarios are added, in which the outlet negative pressure is 4.0 Pa (ventilation_4) and 4.5 Pa (ventilation_5), and we quantitatively analyze the droplet number at different moments in six scenarios. Results show that the local exhaust ventilation system can reduce the number of droplets, which can be seen in Fig. 15. When the negative outlet pressure is 2.5 Pa, the number of moving droplets in the ward reduces by nearly 15% compared with the original situation. Interestingly, as the negative outlet pressure rises from the initial value to 3.0 Pa, more droplets remain in the room than in the original ward. It can be explained that the existence of the local exhaust system promotes turbulent transport, leading to a complete disruption of the droplet cloud and enhancing the dispersion of droplets in the ward. As increasing the outlet negative pressure, we find that the number of droplets staying in the room gradually decreases. When the negative outlet pressure increases to 4.5 Pa, the local exhaust ventilation system can capture and exhaust more droplets than other scenarios. The number of droplets tracked in the ward reduces reduced by nearly 30% compared with the original ward. This is because the mass of the droplets is light, and when the negative outlet pressure value reaches a certain value, droplets caused by a coughing event can be removed more effectively. However, the effect of ventilation on patient comfort remains to be studied.

In addition to the droplets that spread with the air in the ward, a portion of droplets evaporates into water vapor according to Eq. (4-5). Fig. 16 illustrates the number of droplets evaporated in the ward over time. Over time, more droplets evaporate into water vapor and exist in the room in the form of water vapor, which is more conducive to the formation of aerosols. This allows pathogenic microorganisms to remain indoors for a long time, which increases the exposure of COVID-19 to healthcare staffs. The local exhaust system can minimize the number of droplets evaporated in the ward. But the formation of aerosols cannot be avoided.

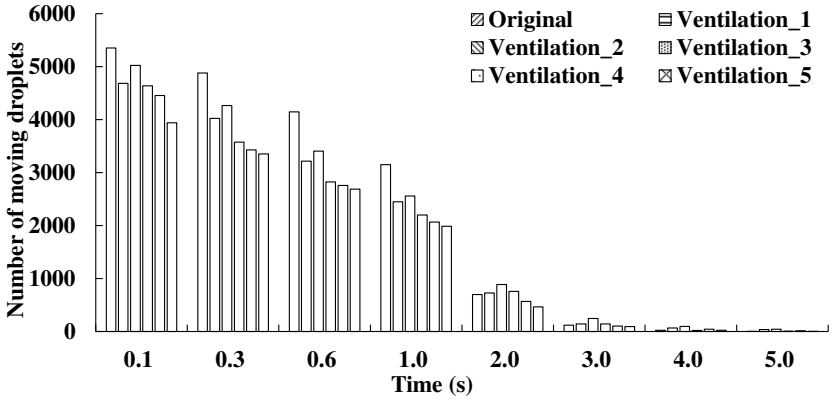

Fig. 15 Number of droplets moving in the ward over time.

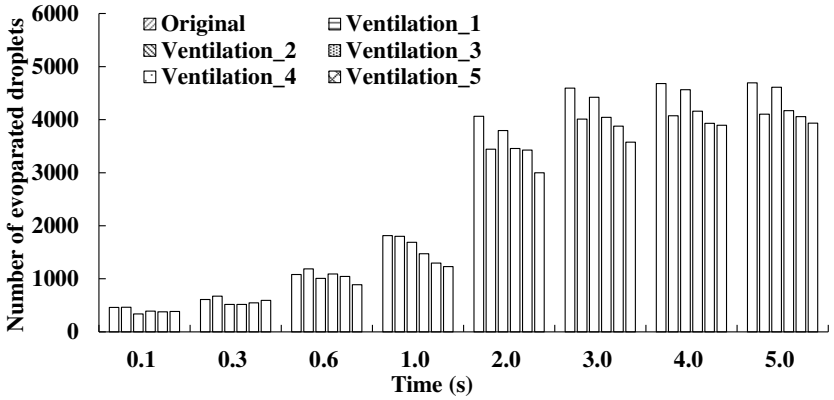

Fig. 16 Number of droplets evaporated in the ward over time.

As for the number of deposited droplets, there are 60.83%, 62.04%, 61.03%, 60.22%, 62.97% and 61.52% of droplets produced by cough deposited on the area around the patient in six scenarios. Fig. 17 illustrates the number of droplets deposited on the patient surface with different diameters. The number of droplets with diameters of 0.01-0.03 mm accounts for nearly 38.1% of the deposited droplets. According to the results, the local exhaust system has no obvious impact on the prevention and control of surface contamination.

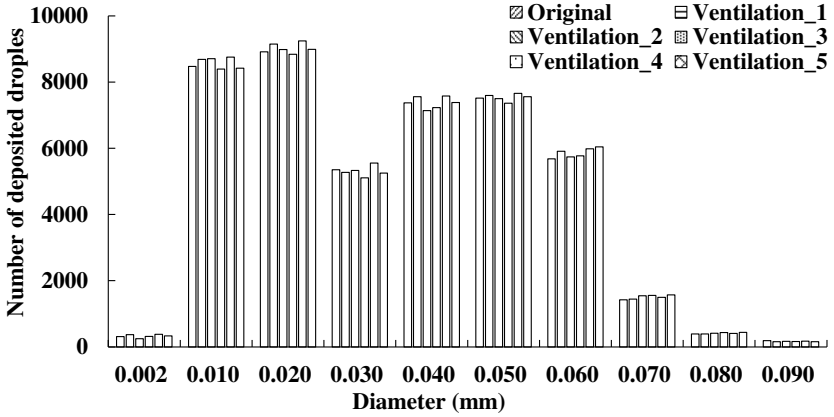

Fig. 17 Number of droplets deposited on the surface of the patient in the ward with different diameters.

Conclusion

In this study, the full-scale geometry of the isolation ward in Wuhan Pulmonary Hospital is modeled and the droplet diffusion process from a coughing event in the ward is simulated. An experiment is conducted to validate the CFD model, and a local exhaust ventilation system is designed to ensure the air quality indoors.

(1) Although the local exhaust ventilation system reduces the number of airborne contaminants, this also leads to a substantial increase in turbulent air motions. Results show that a negative outlet pressure of 2.5 Pa and 3.5 Pa led to a decrease in evaporated droplets and airborne contaminants remaining indoors, and the negative outlet pressure of 3.0 Pa increases the number of droplets tracked in the ward of the excessively turbulent flow. It is found that the number of droplets remaining indoors on the outlet negative pressure is not linear. The exhaust system can effectively

extract contaminants when the negative pressure value is small. But the negative pressure is increased, the local exhaust system promotes turbulent transport, leading to a complete breakup of the droplet cluster and enhancing the dispersion of droplets indoors. The mass of the droplets is light, and when the outlet negative pressure value reaches a certain value, droplets can also be removed effectively.

(2) The local exhaust system can minimize the number of droplets evaporated in the ward. However, the formation of aerosols cannot be avoided.

(3) There are 60.83%, 62.04%, 61.03%, 60.22%, 62.97% and 61.52% droplets produced by cough deposited on the patient surface in six scenarios. According to the results, the local exhaust system has no obvious influence on the prevention and control of surface contamination.

Nevertheless, the simulation in the isolation ward proved that the local exhaust ventilation system allows reducing the number of airborne contaminants remaining indoors. The compound of the contaminant droplets is complicated to simulate in CFD, and the droplets are assumed to be absorbed on the surface when droplets collide with the surfaces. The spread of infectious diseases is complex. Therefore, it is difficult to simulate through the CFD method to restore the real process. The simulation of the simplified model can only provide some reference to analysis on contaminant diffusion in the room.

Acknowledgements The authors would like to thank Wuhan Pulmonary Hospital and Renmin Hospital of Wuhan University for assisting in the completion of the experiment.

Ethics approval and consent to participate Not applicable.

Consent for publication Not applicable.

Author Contributions All authors contributed to the study conception and design. Methodology, Software, data collection and analysis were performed by Yunfei Song, Yuqing Hou and Jiayue Wang. Conceptualization, Supervision and Project administration were performed by Chengqing Yang, Hui Li, Hongbin Chen and Shengnan Shen. The first draft of the manuscript was written by Yunfei Song and all authors commented on previous versions of the manuscript. All authors read and approved the final manuscript.

Funding The authors declare that no funds, grants, or other support were received during the preparation of this manuscript.

Competing Interests The authors declare no competing interests.

Availability of Data and Materials All data generated or analyzed during this study are included in this published article.

Reference

Abraham J, Magi V (1997) Computations of transient jets: RNG *k-ε* model versus standard *k-ε* model. *SAE Technical Papers*, 1442-1452. https://doi.org/10.4271/970885

Al-Benna S (2021) Negative pressure rooms and COVID-19. *Journal of Perioperative Practice*, 31(1-2): 18-23. https://doi.org/10.1177/1750458920949453

ANSI/ASHRAE/ASHE Standard 170-2017 (2017), Ventilation of health care facilities. ASHRAE 170-2017

Bhattacharyya S, Dey K, Paul AR, Biswas R (2020) A novel CFD analysis to minimize the spread

401 of COVID-19 virus in hospital isolation room. *Chaos, Solitons & Fractals,* 139: 110294.
402 https://doi.org/10.1016/j.chaos.2020.110294
403 Bi R, Ali S, Savory E, Zhang C (2021) A numerical modelling investigation of the development of
404 a human cough jet. *Engineering Computations*, https://doi.org/10.1108/EC-12-2020-0705
405 Borro L, Mazzei L, Raponi M, et al. (2020) The role of air conditioning in the diffusion of sars-cov-
406 2 in indoor environments: a first computational fluid dynamic model, based on investigations
407 performed at the Vatican state children's hospital. *Environmental research,* 193: 110343.
408 https://doi.org/10.1016/j.envres.2020.110343
409 Bourouiba L, Dehandschoewercker E, Bush JWM (2014). Violent expiratory events: on coughing
410 and sneezing. *Journal of Fluid Mechanics*, 745: 537-563. https://doi.org/10.1017/jfm.2014.88
411 Cai M, Shen S, Li H, et al. (2016) Study of contact characteristics between a respirator and a head
412 form. *Journal of occupational and environmental hygiene*, 13(3): 60. https://doi.org/10.1080/
413 15459624.2015.1116699
414 Chao CY, Wan MP (2006) A study of the dispersion of expiratory aerosols in unidirectional
415 downward and ceiling-return type airflows using a multiphase approach. *Indoor air*, 16(4):
416 296-312. https://doi.org/10.1111/j.1600-0668.2006.00426.x
417 Chen Q (1995) Comparison of different *k-ε* models for indoor air flow computations. *Numerical*
418 *Heat Transfer, Part B Fundamentals*, 28(3): 353-369. https://doi.org/10.1080/10407799508
419 928838
420 Cho J (2018) Investigation on the contaminant distribution with improved ventilation system in
421 hospital isolation rooms: Effect of supply and exhaust air diffuser configurations. *Applied*
422 *Thermal Engineering*, 148: 208-218. https://doi.org/10.1016/j.applthermaleng.2018.11.023
423 Choi JI, Edwards JR (2012) Large-eddy simulation of human-induced contaminant transport in
424 room compartments. *Indoor air*, 22(1): 77-87. https://doi.org/10.1111/j.16000668.2011.00741
425 .x
426 Davardoost F, Kahforoushan D (2019) Evaluation and investigation of the effects of ventilation
427 layout, rate, and room temperature on pollution dispersion across a laboratory indoor
428 environment. *Environmental Science and Pollution Research*, 26(6): 5410-5421. https://doi.
429 org/10.1007/s11356-018-3977-8
430 Fluent ANSYS (2020). Fluent 2020 R2 User Guide. ANSYS Fluent, Canonsburg
431 Guo, ZD, Wang ZY, Zhang SF, et al. Aerosol and surface distribution of severe acute respiratory
432 syndrome coronavirus 2 in hospital wards, Wuhan, China, 2020 (2020). *Emerging infectious*
433 *diseases*, 26, 1583-1591. https ://doi.org/10.3201/eid26 07.20088 5
434 Gupta JK, Lin CH, Chen Q (2011). Transport of expiratory droplets in an aircraft cabin. *Indoor Air*,
435 21(1): 3-11. https://doi.org/10.1111/j.1600-0668.2010.00676.x
436 Hathway EA, Noakes CJ, Sleigh PA, Fletcher LA (2011) CFD simulation of airborne pathogen
437 transport due to human activities. *Building and Environment*, 46(12): 2500-2511. https://doi.
438 org/10.1016/j.buildenv.2011.06.001
439 Jones RM, Brosseau LM (2015) Aerosol transmission of infectious disease. *Journal of occupational*
440 *and environmental medicine*, 57(5): 501-508. https://doi.org/10.1097/JOM.0000000000000
441 448
442 Ke Z, Oton J, Qu K et al. (2020) Structures and distributions of SARS-CoV-2 spike proteins on
443 intact virions. *Nature*, 588(7838): 498-502. https://doi.org/10.1038/s41586-020-2665-2
444 Kukkonen J, Vesala T, Kulmala M. The interdependence of evaporation and settling for airborne

445 freely falling droplets. *Journal of Aerosol Science*, 1989, 20(7): 749-763. https://doi.org/10.
446 1016/0021-8502(89)90087-6
447 Li H, Leong FY, Xu G, et al. (2020) Dispersion of evaporating cough droplets in tropical outdoor
448 environment. *Physics of Fluids*, 32(11): 113301. https://doi.org/10.1063/5.0026360
449 Li H, Zhong K, Zhai Z (John) (2020) Investigating the influences of ventilation on the fate of
450 particles generated by patient and medical staff in operating room. *Building and Environment,*
451 180: 107038. https://doi.org/10.1016/j.buildenv.2020.107038
452 Lindsley WG, Blachere FM, Beezhold DH, et al. (2016) Viable influenza a virus in airborne particles
453 expelled during coughs versus exhalations. *Influenza and other respiratory viruses*, 10(5): 404-
454 13. https://doi.org/10.1111/irv.12390
455 Liu Y, Li H, Feng G (2017) Simulation of inhalable aerosol particle distribution generated from
456 cooking by Eulerian approach with RNG k–epsilon turbulence model and pollution exposure
457 in a residential kitchen space. *Building Simulation*, 10(1): 35-144. https://doi.org/10.1007/
458 s12273-016-0313-4
459 Liu Y, Ning Z, Chen Y, et al. (2020) Aerodynamic analysis of SARS-CoV-2 in two Wuhan hospitals.
460 *Nature*, 582, 557-560. https ://doi.org/10.1038/s41586-020-2271-3
461 Liu Z, Wang L, Rong R, et al. (2020) Full-scale experimental and numerical study of bioaerosol
462 characteristics against cross-infection in a two-bed hospital ward. *Building and Environment,*
463 186: 107373. https://doi.org/10.1016/j.buildenv.2020.107373
464 Luo H, Liu J, Li C, et al. (2020) Ultra-rapid delivery of specialty field hospitals to combat COVID-
465 19: Lessons learned from the Leishenshan Hospital project in Wuhan. *Automation in*
466 *Construction*, 119: 103345. https://doi.org/10.1016/j.autcon.2020.103345
467 Mao N, An CK, Guo LY, et al. (2020) Transmission risk of infectious droplets in physical spreading
468 process at different times: a review. *Building and Environment*, 107307. https://doi.org/10.
469 1016/j.buildenv.2020.107307
470 Morawska L, Cao J (2020) Airborne transmission of SARS-CoV-2: the world should face the reality.
471 *Environment international*, 139: 105730. https://doi.org/10.1016/j.envint.2020.105730
472 Nicas M, Nazaroff WW, Hubbard A (2005) Toward understanding the risk of secondary airborne
473 infection: Emission of respirable pathogens. *Journal of occupational and environmental*
474 *hygiene*, 2(3): 143-154, https://doi.org/10.1080/15459620590918466
475 Nissen K, Krambrich J, Akaberi D, et al. (2020) Long-distance airborne dispersal of SARS-CoV-2
476 in COVID-19 wards. *Scientific reports*, 10(1): 1-9. https://doi.org/10.21203/rs.3.rs-34643/v1
477 Parienta D, Morawska L, Johnson G R, et al. (2011) Theoretical analysis of the motion and
478 evaporation of exhaled respiratory droplets of mixed composition. *Journal of aerosol science*,
479 42(1): 1-10. https://doi.org/10.1016/j.jaerosci.2010.10.005
480 Song Y, Yang Q, Li H, et al. (2021) Simulation of indoor cigarette smoke particles in a ventilated
481 room. *Air Quality, Atmosphere & Health*, 1-11: 1837-1847. https://doi.org/10.1007/s11869-
482 021-01057-z
483 Wang C, Holmberg S, Sadrizadeh S (2018) Numerical study of temperature-controlled airflow in
484 comparison with turbulent mixing and laminar airflow for operating room ventilation. *Building*
485 *and Environment*, 144: 45-56. https://doi.org/10.1016/j.buildenv.2018.08.010
486 Wei J, Li Y (2015) Enhanced spread of expiratory droplets by turbulence in a cough jet. *Building*
487 *and Environment*, 93: 86-96. https://doi.org/10.1016/j.buildenv.2015.06.018
488 WTO (World Health Organization) (2009) Natural ventilation for infection control in health-care

489 settings. Available at https://www.ncbi.nlm.nih.gov/books/NBK143284/. Accessed January
490 2009
491 WTO (World Health Organization) (2020) Transmission of SARS-CoV-2: Implications for infection
492 prevention precautions. Available at https://www.who.int/news-room/commentaries/detail.
493 Accessed 14 August 2020
494 WTO (World Health Organization) (2021) WHO Coronavirus (COVID-19) Dashboard. Available
495 at https://covid19.who.int/. Accessed 20 January 2022
496 Yakhot V, Orszag SA (1986) Renormalization group analysis of turbulence. I. Basic theory. *Journal*
497 *of scientific computing*, 1(1): 3-51. https://doi.org/10.1007/BF01061452
498 Yao H, Song Y, Chen Y, et al. (2020) Molecular architecture of the SARS-CoV-2 Virus. *Cell*, 183(3):
499 730-738. https://doi.org/10.37473/dac/10.1101/2020.04.
500 Zhang X, Li H, Shen S, Cai M (2015) Investigation of the flow-field in the upper respiratory system
501 when wearing N95 filtering facepiece respirator. *Journal of occupational and environmental*
502 *hygiene*, 13(5):372-382. https://doi.org/10.1080/15459624.2015.1116697
503 Zhu N, Zhang D, Wang W, et al. (2020) A novel coronavirus from patients with pneumonia in china,
504 2019. *New England journal of medicine*, 382(8): 727-733. https://doi.org/10.37473/dac/10.
505 1101/2020.04.07.20057299